Illustrating the Molecular Origin of Mechanical Stress in Ductile Deformation of Polymer Glasses

Xiaoxiao Li, Jianning Liu, Zhuonan Liu, Mesfin Tsige, and Shi-Qing Wang

Phys. Rev. Lett. **120**, 077801 — Published 13 February 2018

DOI: 10.1103/PhysRevLett.120.077801

Illustrating molecular origin of mechanical stress in ductile deformation of polymer glasses

Xiaoxiao Li, Jianning Liu,[†] Zhuonan Liu, Mesfin Tsige and Shi-Qing Wang

Abstract

New experiments show that tensile stress vanishes shortly after pre-yield deformation of polymer glasses while tensile stress from post-yield stays high and relaxes on much long time scales, thus hinting at a specific molecular origin of stress in ductile cold drawing: chain tension rather than intersegmental friction. Molecular dynamics simulation based on a coarse-grained model for polystyrene confirms the conclusion that the chain network plays an essential role, causing the glassy state to yield and to respond with a high level of intrachain retractive stress. This identification sheds light on the future development regarding improved theoretical account for molecular mechanics of polymer glasses and the molecular design of stronger polymeric materials to enhance their mechanical performance.

PACS numbers: 83.85.St; 81.05.Kf; 83.60.Df

[†] Liu made equally important contributions as the first author did.

High molar-mass polymers are complicated, especially strongly correlated many-body systems. Their mechanical responses to large deformation are challenging to describe both in their melt state where chain entanglement is a dynamic topological consequence of intermolecular uncrossability and in their glassy state where inter-segmental interactions overwhelms the role of the chain network. Unlike any other types of materials such as ceramics and metals, polymeric materials are highly stretchable in their liquid state (rubber bands being an example) and drawable in their glassy state, e.g., capable of doubling the equilibrium length. Above the glass transition temperature T_g, melts' high rubbery extensibility is widely understood in terms of a phantom network of Gaussian chains that can be stretched multiple times their original sizes before becoming straightened. However, below T_g, a sufficiently high molecular weight does not guarantee ductile drawing. Although the concept of chain entanglement has been invoked for decades [1,2] to acknowledge the prerequisite of high molecular weight for ductility, it was unclear [3-5] just how polymer entanglement would afford a glassy polymer the unique properties such as the extraordinary ductility demonstrated by bisphenol A polycarbonate (PC). Despite its high glass transition temperature T_g at 145 ^{o}C, PC can be cold drawn to a great extent without brittle fracture even at –120 ^{o}C.

For ductile polymer glasses, Kramer's criticism [6] on a conventional view to regard strain hardening as due to “rubber elasticity” provided the new impetus to evaluate intermolecular contributions to the macroscopic stress. Several subsequent studies [7-14] supported the view that (a) post-yield deformation of polymer glasses is largely dissipative, (b) changes in intersegmental packing can lead to an increase of stress with strain and (c) even low-molecular weight polymer glass can show strain hardening.

Initial stress growth in melt deformation is widely regarded as due to intrachain retraction forces of stretched strands in the entanglement network. The intrachain forces can make a melt-stretched polymer to undergo complete elastic recoil. For polymer glasses it is far less clear whether or not intrasegmental forces make a dominant contribution to the tensile stress in the post-yield extension (ductile drawing). After significant ductile cold-drawing well below the glass transition temperature T_g and unloading without external constraint, a deformed polymer glass would soon stop any visible contraction and retain its extended length during the sequent days of storage at the cold-drawing temperature. There would be no macroscopic retractive stress. On the other hand, upon annealing of such a cold-drawn glassy polymer above the storage temperature but still well below T_g, retractive stress can develop in time [15-17].

In this work, we design several experiments to explore the molecular origin of macroscopic stress in both pre-yield and post-yield regimes and verify the emerging picture [18] using molecular-dynamics computer simulation. The challenge to explore the molecular origin of stress during ductile deformation well below T_g stems from the fact that the alpha relaxation time τ_α is inconveniently long. Fig.1 shows that at room temperature the stress relaxation after post-yield extension of PC is extremely slow at long times, as slow as that from pre-yield deformation. By conducting the experiment at higher temperatures, Fig. 2 shows that τ_α becomes ca. 1000 s at 135 ^{o}C.

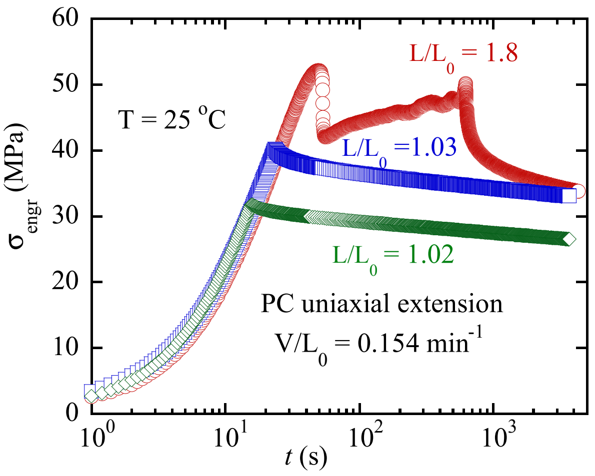

Figure 1

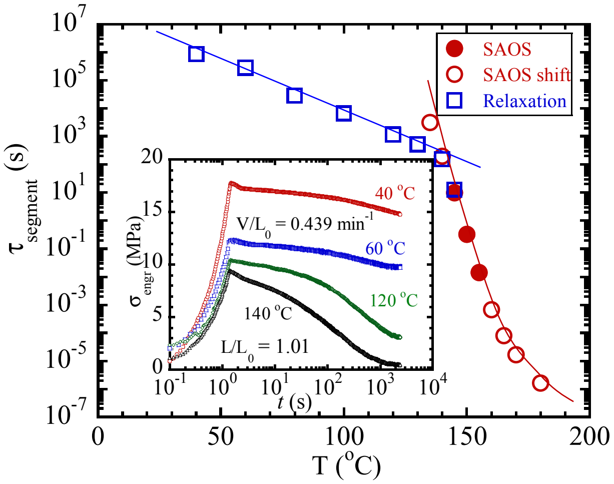

Figure 2

Fig. 1 Tensile (engineering) stress during and after uniaxial extension of PC to draw ratios L/L_0 = 1.02, 1.03 (pre-yield) and 1.8 (post-yield) at a crosshead speed V = 6 mm/min, with an initial specimen length L_0 = 39 mm.

Fig. 2 Alpha segmental relaxation time τ_α determined from both SAOS measurements and KWW fitting to the stress relaxation (inset). Filled circles are directly obtained from the reciprocal of the third crossover frequency ω_α. Open circles were obtained based on the WLF shifting of ω_α. The squares were the average relaxation time τ from the KWW fitting to the relaxation data in the inset that shows the tensile stress during and after extension of PC to draw ratio L/L_0 = 1.01 at a crosshead speed V = 6 mm/min at four different temperature below T_g from 40 to 140 °C.

In this work, we explore the molecular origin of mechanical stress during ductile extension of polymer glasses by characterizing the stress relaxation behavior in both pre-yield and post-yield regimes, at 10 to 15 degrees below T_g. The diamonds in Fig. 3 show that the tensile stress from pre-yield vanishes in 60 min for PC at 135 ^{o}C. This stress decay can conventionally be explained in terms of segmental alpha relaxation and reveals an alpha relaxation time τ_α on the order of several minutes, as indicated in Fig. 2. During the cold drawing, beyond the elastic pre-yield regime, shear yielding occurs, leading to the stress decline, followed by necking and neck front propagation during which the tensile stress remains constant. The stress relaxation behavior from the post-yield regime is remarkably different as shown by the circles in Fig. 3, where the inset presents the stress vs. strain curve, along with the three vertical arrows to indicate the three stages at which the stress relaxation test begins. Specifically, in contrast to the stress relaxation from pre-yield elastic deformation (diamonds), the stress relaxation at the yield point (squares) reveals some residual stress at long times; moreover, there is significant stress at long times for L/L_0 = 1.7 (circles - after completion of necking).

Recent consensus suggests [14] that mechanical stress during plastic deformation is dominantly dissipative, leading to the expectation that the circles in Fig. 3 should approach zero as fast as the diamonds: If the stress is generated by intersegmental interactions, the stress should vanish in 60 min via the alpha process as it does in pre-yield regime; moreover, much of the initial rapid stress decline should also involve intermolecular repacking. However, unexpectedly, not only does the stress stays high on the pertinent time scale of 60 min, even the squares remain non-vanishing after 60 min of relaxation from the yield point.

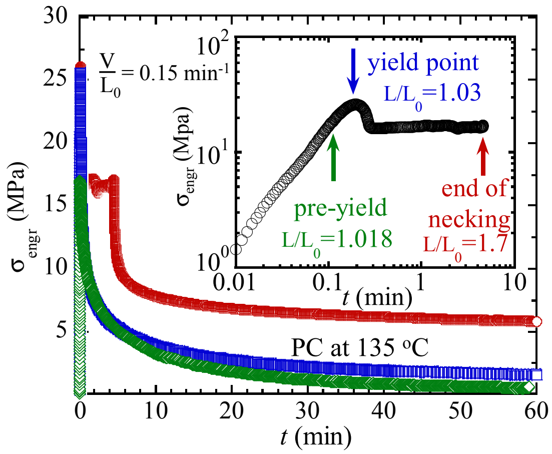

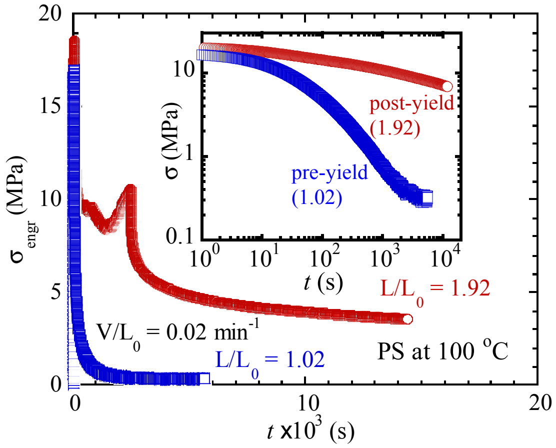

Figure 3

Figure 4

Fig. 3 Tensile (engineering) stress during and after drawing of PC to draw ratios L/L_0 = 1.018 (pre-yield), 1.03 and 1.7 (post-yield, right after necking is completed) at 135 °C and a crosshead speed V = 6 mm/min, with L_0 = 39 mm. Stress provided by pre-yield drawing vanishes while stress from post-yield drawing remains high on the same time scale. The inset shows the stress variation with time to indicate with the three vertical arrows of different colors (corresponding to the colors (online) in the main figure) when the stress relaxation took place.

Fig. 4 Engineering stress during and after drawing of PS to draw ratios L/L_0 = 1.02 (pre-yield) and 1.92 (post-yield after the end of necking) at a crosshead speed V = 1.8 mm/min, with L_0 = 90 mm. Similar to Fig. 1, stress from post-yield drawing survives at long times. The stress relaxation in the inset shows contrasting characteristic time scales: the stress relaxation is much slower from post-yield deformation.

To determine whether the observations in Fig. 3 are universal, we carried out similar extensional drawing of glassy polystyrene. The polystyrene in the present study has T_g = 103 °C. Therefore, we carried out the stress relaxation at T = 100 °C from pre-yield at L/L_0 = 1.02 as well as post-yield at L/L_0 = 1.92 beyond the completion of necking. As shown in Fig. 4, the stress relaxation from pre-yield extension occurs on a time scale of several hundred seconds. In contrast, the stress remains high after post-yield extension at L/L_0 = 1.92 even after several thousand seconds. The inset of Fig. 4

shows that the pre-yield stress relaxation is rapid on time scales of 10^2 s while the post-yield relaxation is considerably slower on all time scales. How could the stress relaxation (circles) be so slow even initially, much slower than that prescribed by the alpha process? What does this phenomenon of slow stress relaxation imply regarding the molecular origin of the tensile stress during post-yield drawing? Ideas such as intermolecular cooperativity [19] and Eyring activation [20,21] would suggest that the dynamics should always be faster after post-yield deformation, in contradiction to such data as shown in the inset of Fig. 4.

Given the importance of these questions, it is necessary to verify the characteristic revealed in Fig. 4 for PS. According to a recently published study [22], the initial stress relaxation from post-yield deformation of PC occurs on time scales in proportion to the reciprocal of the deformation rate invoked to produce the post-yield deformation. This study asserted, consistent with the recent molecular model for yielding of polymer glasses [18], that a) the mechanical stress in post-yield should have a significant intrasegmental contribution and b) the molecular mobility produced by the post-yield deformation governs how quickly intrasegmental component relaxes. Thus, to confirm the universality of Fig. 4, we subject PC to both pre-yield and post-yield extension using a sufficiently small extensional rate and found similar data. As shown in Supplementary Material, Fig. S.4 indicates that the stress decay occurs on the time scale of 10^2 s for step extension at $L/L_0 = 1.01$ in the pre-yield regime but the stress hardly decreases on the same time scale after cold drawing to a ratio of $L/L_0 = 2.1$. We are led to conclude that the stress present during and after ductile drawing is not intersegmental because it did not and could not relax on the alpha relaxation time scale. In particular, we speculate that at high draw ratios the tensile stress arises from stretching of the chain network.

In the glassy state, after large ductile deformation, bond orientation and stretching may keep the retractive stress high until collective movements take place on much longer time scales than the time scale associated with the monomeric alpha process. Since the alpha process is not collective, it may not be effective to cause conformational changes that require structural adjustment on length scales considerably larger than the monomer scale. Therefore, two specific features have led to the conclusion that in the post-yield drawing the mechanical stress is intrasegmental in origin. First, the tensile stress still remains high at long times. Second, the stress decay after significant post-yield extension can be much slower during every stage of relaxation than the stress relaxation from pre-yield deformation. This conclusion concerning the microscopic origin of stress pertains to many issues in the literature including a) the essence of strain hardening [7-14], b) elastic deformation and internal energy buildup in post-yield regime [23,24], c) "anelasticity" associated with hidden stress in the glassy state. Although stress due to intersegmental interactions, e.g., stretching of van der Waals bonds, can relax through alpha processes, the segmental relaxation is ineffective to remove chain tension produced during ductile drawing. Thus, the present study of stress relaxation has clarified the origin of mechanical stress during post-yield extension. Formation of a chain network in glassy state requires intersegmental interactions – chain uncrossability is inherently an intermolecular effect. However, for a strained chain network to relax its stress requires structural adjustment on length scales significant larger than the monomer size. Thus, the stress from post-yield deformation stays high on the alpha time scale, on which comparably high pre-yield stress vanishes. Although dynamic and structural heterogeneities [25,26] are expected to be present, their existence does not offer a straightforward account for the observed remarkable difference in pre-yield and post-yield stress relaxation. Nevertheless, it would be desirable for future studies to explore how heterogeneities may affect stress relaxation on both short and long time scales.

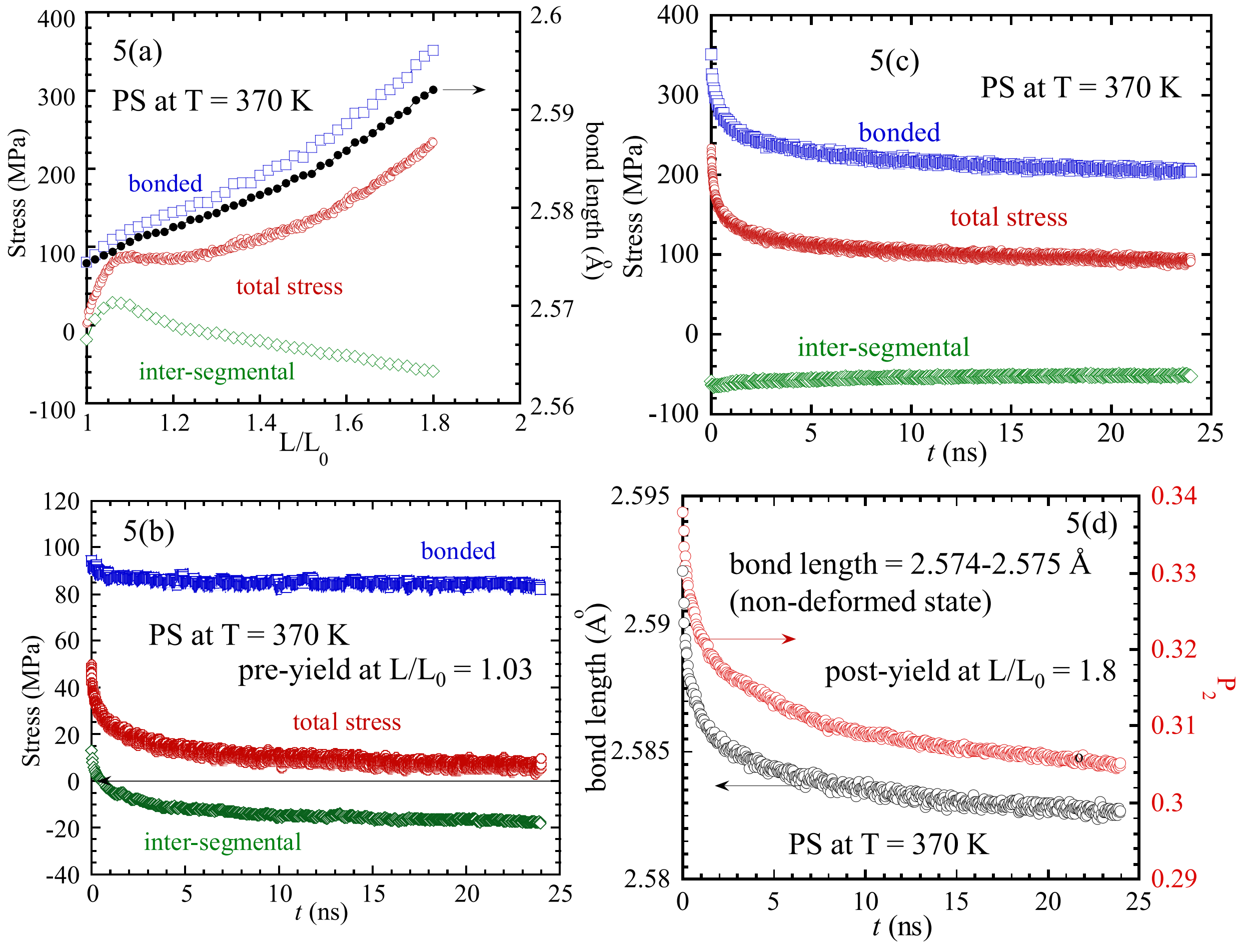

Fig. 5 (a) Different components of stress and bond lengthening (right-hand-side Y axis) during drawing of PS at 370 K, obtained from molecular dynamics simulation involving Hencky rate 0.5/ns. (b) Relaxation of different stress components from pre-yield drawing to $L/L_0 = 1.03$, where the stress decomposition is illustrated in (a) at $L/L_0 = 1.03$. (c) Relaxation of different stress components from post-yield drawing to $L/L_0 = 1.8$. (d) Bond length and bond orientation in terms of P_2 both decreases with time during the stress relaxation.

To further illustrate the molecular origin of stress, using a coarse-grained model for polystyrene (PS) [27], we carried out molecular dynamics simulation to examine the stress responses during and after cold drawing (uniaxial extension). We found from the simulation that before yielding both the covalent bonds and LJ bonds are stretched, resulting in a retractive stress; in post-yield regime, for PS of molecular weight equal to 50,000 g/mol, the buildup of the tensile stress stems from the resistance of the chain network to the extension. Beyond yielding, the intersegmental interactions gradually turn compressive. Fig. 5(a) shows the decomposition of the stress as a function of the draw ratio L/L_0, where appreciable bond stretching accompanies the growing tensile stress. Thus, the simulation result supports the conclusion drawn from the experimental findings in Figs. 3 to 5 that the post-yield extension produces substantial conformational changes associated with stretching of a chain network. Details about the coarse-grained model and simulation protocol can be found in the Supplemental Material[28] where we show in Fig. S.6 that the molecular origin of stress is both enthalpic associated with the bond lengthening and entropic due to the bond orientation.

The molecular dynamics simulation results also support the interpretation of the experimental data in Figs. 3 to 5(a)-(d) concerning why stress relaxation from pre-yield deformation could be much faster than that from post-yield: The origin of stress is largely different between pre-yield and post-yield. Specifically, Fig. 5(b) shows that the fast stress decay from pre-yield occurs due to the available segmental mobility. As the intersegmental packing recovers toward its non-deformed state where the intersegmental stress is compressive, the intersegmental stress changes from being initially retractive to compressive (negative). The bonded stress remains unchanged. In contrast, Fig. 5(c) shows that after post-yield drawing the initial rapid stress decay is dominantly intrasegmental in origin because the intersegmental component of the stress hardly declined. At long times, the retractive stress stays high because covalent bonds still remain significantly stretched and oriented, as shown in Fig. 5(d).

To more clearly illustrate the microscopic origin of the tensile stress during and after cold drawing, we perform additional analysis to visualize the buildup of chain tension upon cold drawing to $L/L_0 = 1.8$. Fig. 6 shows strands whose bonds have been stretched to a bond length of at least 2.6 Å and remained so stretched 4 ns after the onset of the stress relaxation. The global retractive stress partially stems from these taut strands that permeate from one end of the system to the other end. Fig. 6 indicates that some of these load-bearing strands still survive after significant relaxation at *t = 24* ns. Such taut states have been observed in previous MD simulations [8,9].

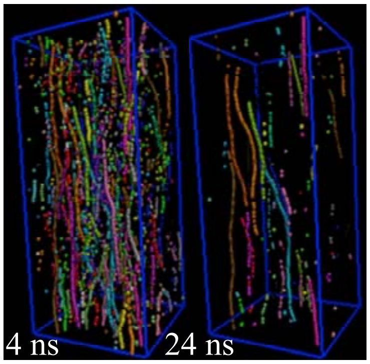

Fig. 6 States of bond stretching during stress relaxation of PS 4 and 24 ns after tensile extension to a draw ratio of L/L_0 = 1.8 at 370 K. All bonds with length 2.6 Å or longer are shown in the left and right panel respectively. The different colors (online) represent different strands containing such stretched

bonds. The equilibrium bond length is 2.574-2.575 Å. At 4 ns there are many more such load-bearing strands than at 24 ns. These strands stem from one end of the system to the other.

In conclusion, we show by experiment and MD simulation that deformation of a chain network at the bond level (leading to bond orientation and stretching) is the leading cause of the emergent tensile stress during ductile extension. During stress relaxation from post-yield extension, orientation is unable to relax on the alpha time scale. MD simulation confirms that the tensile extension is retractive and intrasegmental in origin due to orientation and stretching of the backbone bonds. It remains an intriguing question whether non-polymeric glasses such as colloidal glasses[29] could ever display slower stress relaxation from post-yield deformation than from pre-yield deformation. This work is supported, in part, by the National Science Foundation (DMR- 1609977).

References

[1] R. N. Haward, Macromolecules **26**, 5860 (1993).

[2] H. G. H. van Melick, L. E. Govaert, and H. E. H. Meijer, Polymer **44**, 2493 (2003).

[3] R. N. Haward and R. J. Young, *The Physics of Glassy Polymers* (Springer Netherlands, 1997).

[4] I. M. Ward and J. Sweeney, *Mechanical properties of solid polymers, 3rd* (John Wiley & Sons, Ltd., Chichester, UK, 2012).

[5] A. S. Argon, *The Physics of Deformation and Fracture of Polymers* (Cambridge University Press, 2013).

[6] E. J. Kramer, J. Polym. Sci., Part B: Polym. Phys. **43**, 3369 (2005).

[7] A. V. Lyulin, B. Vorselaars, M. A. Mazo, N. K. Balabaev, and M. A. J. Michels, Europhys. Lett. **71**, 618 (2005).

[8] R. S. Hoy and M. O. Robbins, J. Polym. Sci. Pt. B-Polym. Phys. **44**, 3487 (2006).

[9] R. S. Hoy and M. O. Robbins, Phys. Rev. Lett. **99**, 117801 (2007).

[10] R. S. Hoy and M. O. Robbins, Physical Review E **77**, 031801 (2008).

[11] B. Vorselaars, A. V. Lyulin, and M. A. J. Michels, J. Chem. Phys. **130**, 074905 (2009).

[12] K. Chen and K. S. Schweizer, Phys. Rev. Lett. **102**, 038301 (2009).

[13] B. Vorselaars, A. V. Lyulin, and M. A. J. Michels, Macromolecules **42**, 5829 (2009).

[14] R. S. Hoy, J. Polym. Sci. Pt. B-Polym. Phys. **49**, 979 (2011).

[15] R. D. Andrews, J. Appl. Phys. **26**, 1061 (1955).

[16] D. G. Legrand, J. Appl. Polym. Sci. **16**, 1367 (1972).

[17] S. Cheng and S.-Q. Wang, Phys. Rev. Lett. **110**, 065506 (2013).

[18] S.-Q. Wang, S. Cheng, P. Lin, and X. Li, J. Chem. Phys. **141**, 094905 (2014).

[19] S. Matsuoka and X. Quan, Macromolecules **24**, 2770 (1991).

[20] H. Eyring, J. Chem. Phys. **4**, 283 (1936).

[21] K. Chen and K. S. Schweizer, Macromolecules **41**, 5908 (2008).

[22] J. N. Liu, P. P. Lin, X. X. Li, and S. Q. Wang, Polymer **81**, 129 (2015).

[23] O. A. Hasan and M. C. Boyce, Polymer **34**, 5085 (1993).

[24] P. P. Lin, J. N. Liu, and S. Q. Wang, Polymer **89**, 143 (2016).

[25] M. D. Ediger, Annu. Rev. Phys. Chem. **51**, 99 (2000).

[26] S. C. Glotzer, J. Non-Cryst. Solids **274**, 342 (2000).

[27] D. D. Hsu, W. Xia, S. G. Arturo, and S. Keten, Macromolecules **48**, 3057 (2015).

[28] See Supplemental Material [url] for details about the coarse-grained model and simulation protocol as well as experiment details which includes Refs. [30-36].).

[29] M. Ballauff *et al.*, Phys. Rev. Lett. **110**, 215701 (2013).

[30] K. Schröter, S. A. Hutcheson, X. Shi, A. Mandanici, and G. B. McKenna, J. Chem. Phys. **125**, 214507 (2006).

[31] R. Kohlrausch, Annalen der Physik **167**, 179 (1854).

[32] G. Williams and D. C. Watts, Transactions of the Faraday Society **66**, 80 (1970).

[33] J. Hagenah, G. Meier, G. Fytas, and E. Fischer, Polym. J. **19**, 441 (1987).

[34] M. Cardona, R. V. Chamberlin, and W. Marx, Annalen der Physik **16**, 842 (2007).

[35] K. Paeng, S. F. Swallen, and M. D. Ediger, J. Am. Chem. Soc. **133**, 8444 (2011).

[36] S. Plimpton, J. Comput. Phys. **117**, 1 (1995).